

Anatomical and functional imaging of neurons using 2-photon laser scanning microscopy

W. Denk *, K.R. Delaney, A. Gelperin, D. Kleinfeld, B.W. Strowbridge, D.W. Tank, R. Yuste

Biological Computation Research Department, AT&T Bell Laboratories, Murray Hill, NJ 07974, USA

Received and accepted 28 June 1994

Abstract

Light scattering by brain tissue and phototoxicity are major obstacles to the use of high-resolution optical imaging and photo-activation ('uncaging') of bioactive compounds from inactive ('caged') precursors in intact and semi-intact nervous systems. Optical methods based on 2-photon excitation promise to reduce these obstacles (Denk, 1994; Denk et al., 1990, 1994). Here we show a range of imaging modes based on 2-photon laser scanning microscopy (TPLSM) as applicable to problems in neuroscience. Fluorescence images were taken of neurons labeled with ion-sensitive and voltage-sensitive dyes in invertebrate ganglia, mammalian brain slices, and from the intact mammalian brain. Scanning photochemical images with whole-cell current detection (Denk, 1994) show how the distribution of neurotransmitter receptors on the surface of specific cells can be mapped. All images show strong optical sectioning and usable images can be obtained at depths greater than 100 μm below the surface of the preparation.

Keywords: Microscopy, 2-photon laser scanning; Light scattering; Phototoxicity; Receptor, neurotransmitter

1. Introduction

Light at visible wavelengths is scattered particularly strongly by nervous tissue. For example, in the mammalian brain slice preparation, the dendrites of CA1 hippocampal pyramidal neurons filled with the fluorescent calcium indicator fura-2 can only be clearly resolved using conventional fluorescence microscopy if the dendrite lies within a few tens of micrometers of the surface (Regehr and Tank, 1992). This strong scattering makes high-resolution measurements throughout the dendritic tree difficult in these preparations except when, as in few cell types, most notably the Purkinje cell, a planar dendritic tree can be oriented parallel to the slice surface (Ross and Werman, 1987; Tank et al., 1988). For a depth beyond several tens of micrometers, scattering at the shorter visible wavelengths is so strong that photon propagation resembles diffusion, which precludes the formation of a focus. In vivo measurements with spatial resolution sufficient to resolve dendrites have only been reported from large neurons in invertebrate preparations (Egelhaaf et al., 1993; Sobel and Tank, 1994).

Confocal microscopy can dramatically improve the spatial resolution and background rejection of images in such highly scattering preparations (see the article by G. Augustine, this issue). However, several properties of confocal microscopy and optical probe chemistry combine to limit the ultimate usefulness of the method in brain tissue (Tsien and Waggoner, 1992). The first is that the vast majority of anatomical tracers, fluorescent ion concentration indicators and voltage-sensitive dyes need to be excited with green, blue, or near UV light if single-photon absorption is used as in conventional confocal microscopy. Scattering is strong at these wavelengths leading to a diversion of light from the focus. The second is that background discrimination in confocal microscopy depends on the fact that only light emanating from the focal region is selected by a conjugate pinhole before the light detection device. Thus, in the presence of scattering, only a small fraction of the fluorescent light originally generated in the focus-voxel is collected, reducing the signal-to-noise ratio. Neither of these two effects would limit achievable signal-to-noise ratios if the intensity of the excitation source could be increased to compensate for light loss. But, in most cases, phototoxicity severely restricts such increases; in fact, it is almost always phototoxicity that

* Corresponding author.

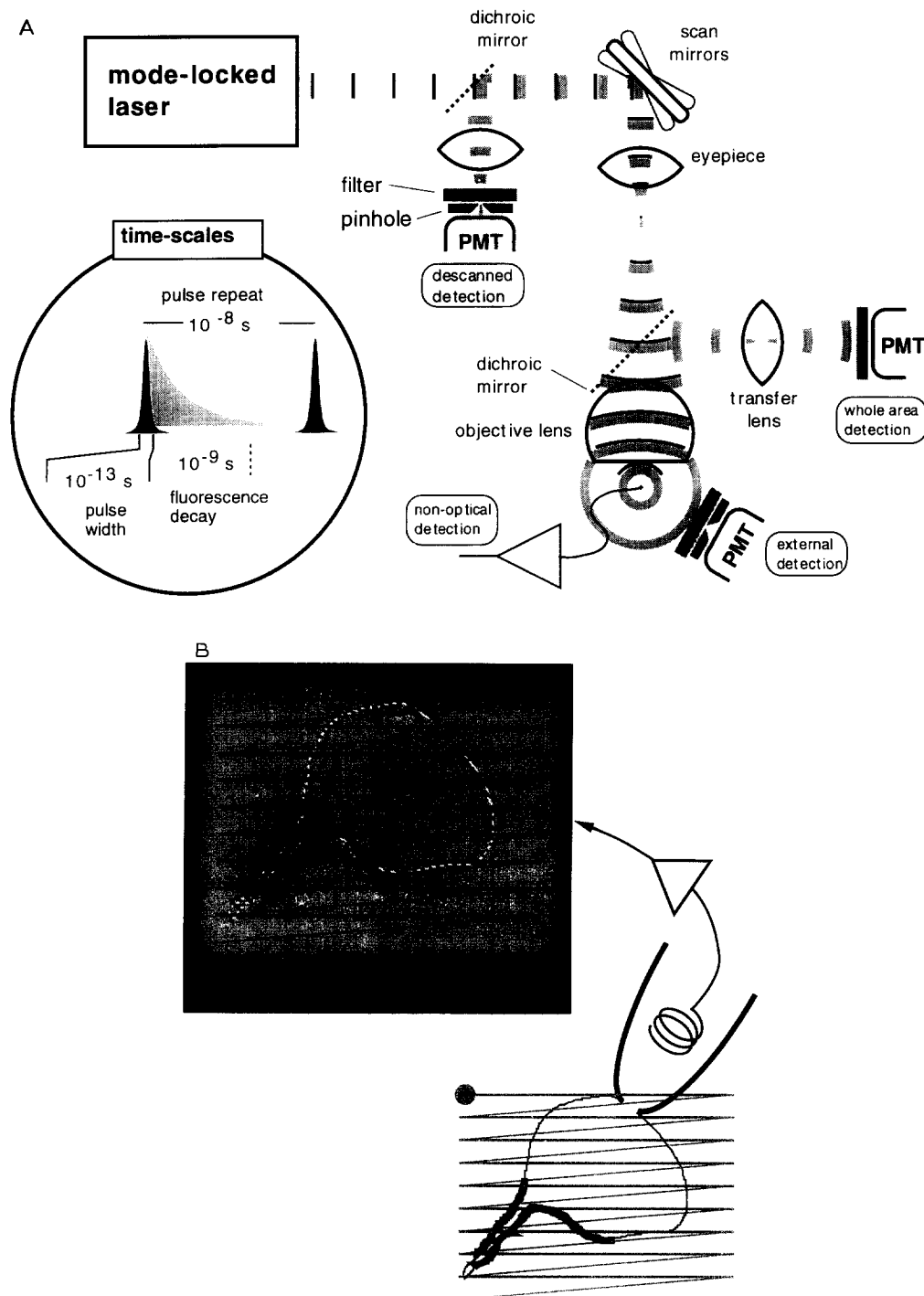


Fig. 1. A: schematic diagram of a TPLSM illustrating the different detection possibilities. The beam of a mode-locked Ti-Sapphire laser (or colliding pulse mode locked dye laser for uncaging) producing a 100 fs pulse every 10 ns is focused to a diffraction limited spot using a microscope objective. Using the same scanning instrumentation as in a confocal laser scanning microscope the beam is rastered across the sample. The emitted fluorescence can be detected in several different ways: (1) by descanning, using the same detector as in the confocal setup, (2) by collecting all photons reentering the objective (preferred if maximum signal collection is required), and (3) externally, if the objective lens does not pass the emitted light or to collect light otherwise lost. Fluorescence images presented here were taken in whole area epi-fluorescence mode. B: principle of SPM as used to map the distribution of neurotransmitter receptors on the cell surface. The amplified whole-cell current (also shown schematically in Fig. 1A) is used to modulate pixel brightness while the excitation beam that is used to uncage a neurotransmitter is scanned across the specimen. Because 2-photon excitation produces optical sectioning, a 3-dimensional map (Fig. 6) can be produced by an appropriate combination of XY scanning of the beam with changes in focus (Z direction).

limits the achievable spatial and temporal resolution in single-photon confocal microscopy. Furthermore, because excitation light is absorbed equally in planes above and below the focal plane phototoxicity occurs throughout the preparation (Tsien and Waggoner, 1992; Denk et al., 1994).

Without giving up any of the depth discrimination of 1-photon confocal microscopy, 2-photon excitation (without confocal detection) by a focused laser beam alleviates these problems in several ways. First, by virtue of the quadratic dependence of the absorption on the local intensity, which also account for the optical sectioning properties, phototoxicity and photobleaching are virtually absent outside the focal slice (Denk et al., 1990, 1994; Stelzer et al., 1994). Second, since optical resolution and sectioning are achieved during excitation, fluorescent photons can contribute to the signal even if they are scattered. These photons would be lost in confocal microscopy because they would not pass through the pinhole.

This is the reason why in scattering specimens photo-damage even in the focal slice is reduced by using 2-photon excitation. Furthermore, 2-photon excitation means that the excitation wavelength is roughly doubled from the UV or blue/green into the red or infrared regime where scattering is considerably reduced and hence optical penetration improved. Finally, signal loss due to scattering can now be compensated by increasing the excitation power without an increase in phototoxicity, assuming, however, negligible 1-photon absorption at the longer excitation wavelength and an overall detection probability for fluorescent photons that does not depend on the focal depth.

Our interest in exploring 2-photon microscopy for imaging neurons stems from the expected increase in optical penetration without increased phototoxicity. The greater transparency of many intact and semi-intact nervous system preparations in the red and near IR has not been studied extensively in a systematic way (for some data see Svaasand and Ellingsen, 1983) but it forms the basis of several previously reported applications. For example, Nomarski imaging of mammalian brain slice with an IR illuminator and IR imaging device provides excellent visibility of neuronal dendrites and soma several hundred micrometers below the cut surface of the mammalian brain slice (MacVicar, 1984; Dodt, 1992, 1993; Dodt et al., 1993). Similarly, the IR transparency of the intact mammalian brain is high enough that trans-cranial spectroscopy can be performed (Jobsis, 1977). That photobleaching is limited to the focal slice with 2-photon excitation should, for cells with appreciable out of plane volume, greatly prolong the available observation time. The collection efficiency of light from excited probe molecules is increased along with it the signal-to-noise ratio because the fluorescent light from the voxel ex-

cited at a particular point during the raster scan does not have to be refocused onto a pinhole and because fewer lossy optical surfaces intervene (Fig. 1A). Furthermore, the optical design is simplified and the periodic precision alignment that confocal systems require is eliminated.

In Section 2 we describe results of our initial attempts at imaging individual neurons and ensembles of neurons using TPLSM. The optical sectioning capabilities are first demonstrated in images of voltage-sensitive dye-stained neurons in an olfactory ganglion in the terrestrial slug *Limax maximus*. The high spatial resolution of the TPLSM is then shown using images of dendrites and synaptic spines belonging to neurons in brain slices from rat hippocampus and turtle cortex labeled by intracellular injection of ion-sensitive indicators. Micrometer-sized structures are resolved more than 100 μm below the slice surface. Finally, high-resolution images of mammalian brain slice and of rat parietal cortex in vivo that were stained with voltage-sensitive dye are presented.

Another application where the optical sectioning capabilities of 2-photon excitation by a focused laser beam may prove very valuable is the 'uncaging' of bioactive compounds such as neurotransmitters and second messengers with high spatial resolution (Denk, 1994). The resulting technique could be called scanning photochemical microscopy (SPM). While direct optical excitation (Fork, 1971; Farber and Grinvald, 1983) and uncaging (Callaway and Katz, 1993; article by Katz in this issue) is possible with 1-photon absorption using a scanning laser, no optical sectioning is attainable, since, unlike in confocal detection of fluorescence, the elicited signal can not be used for additional spatial localization. In general, scanning microscopies are based upon the measurement of a functional signal (typically a measurement of some physical quantity, such as current) from a preparation as a probe or laser beam is raster-scanned across an object. In the first SPM images, the functional signal was intracellular transmembrane current measured with whole-cell patch techniques recorded as neurotransmitter receptors were activated by 2-photon excitation of caged neurotransmitter (Denk, 1994). In Section 3, we review how SPM has been used to produce high spatial resolution images of the distribution of neurotransmitter receptors on the cell surface and discuss how it could be used to map neural circuits.

2. Anatomical and functional 2-photon fluorescence microscopy

We explored the use of TPLSM in brain tissue with the apparatus sketched in Fig. 1A. Excitation light was provided by a mode-locked Ti:Sapphire laser (NJA-1;

Clark Instrumentation) operating at 90 MHz with \approx 100 fs pulse width pumped with a 6 W Argon CW laser (Innova 310; Coherent). Excitation light was focused onto the sample through a water immersion lens to a sub-micrometer diffraction limited spot while scanning was performed using a heavily modified commercial laser scanning microscope (Denk, 1994) (MRC600; Biorad). The average power at the sample was typically 30–50 mW. Emitted light was collected through the same lens used for excitation (epi-fluorescence mode), separated from the excitation light using a dichroic splitter (DLHS coating 800 nm; 340485, Spindler and Hoyer) and bandpass filtered depending on the emission wavelength (BG 18/BG38; Schott), and detected with a photomultiplier tube (R9836; Hamamatsu). Image acquisition, storage, processing, and display were performed using modified commercial software (Comos/SOM programs; Biorad).

2.1. Fluorescence imaging of voltage-sensitive dye-labeled neurons in the procerebral lobe of *L. maximus*

The procerebral (PC) lobe of the cerebral ganglion of the terrestrial slug *L. maximus* contains approximately 100,000 interneurons. The neuronal somata are arranged in a discrete layer surrounding a dense neuropil. Cells in the PC lobe undergo an intrinsic 0.7 Hz oscillation in membrane potential (Gelperin and Tank, 1990) that is easily measured as an oscillation in extracellular field potential. The oscillation can also be optically measured using voltage-sensitive dyes (Delaney et al., 1994), and its frequency and amplitude is an indication of the physiological state of a PC lobe preparation.

Surgically isolated PC lobes were labeled with the voltage-sensitive dye di-4-ANEPPS by bath application, as described (Delaney et al., 1994). Di-4-ANEPPS has

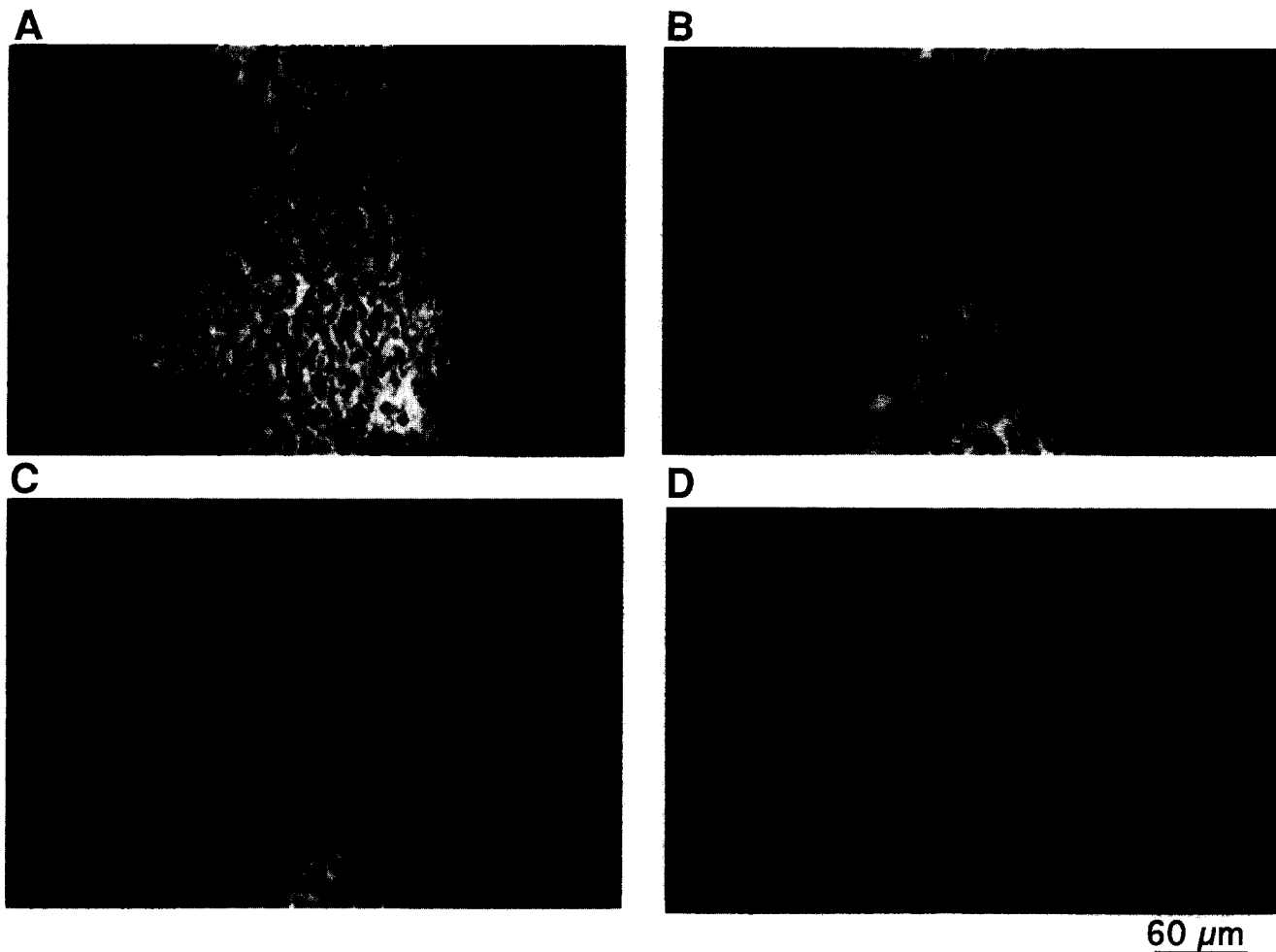


Fig. 2. Fluorescence images of the isolated central olfactory organ (procerebral lobe) of the terrestrial mollusc *L. maximus*. The preparation was stained with the voltage-sensitive dye di-4-ANEPPS as described in the text. Four optical sections taken with the TPLSM ($\lambda = 860$ nm; Zeiss $63\times/0.9$ NA water-immersion objective) at different depths (30, 50, 70, and 100 μm for sections A,B,C and D) below the surface of the lobe are shown. Dense neuropil was observed at greater depths. The estimated thickness of each optical section is about 1 μm .

an 1-photon absorption band with a maximum near 470 nm and a full-width-half maximum (FWHM) of ≈ 110 nm. A set of TPLSM images of the PC lobe excited at 860 nm is shown in Fig. 2. The pixel dimension was $0.4 \times 0.4 \mu\text{m}$ (768×512 pixels) and the dwell-time per pixel was $6 \mu\text{s}$ (3 s/image). These 4 images are representative of a complete set of optical sections taken in intervals of $10 \mu\text{m}$ progressing from the surface of the lobe through the cell body layer and into the neuropil. Four sections from the cell body layer are shown. The dark round circles delimited by a bright ring of fluorescence are cell bodies. Most of the sections show cells $7\text{--}9 \mu\text{m}$ in diameter. Larger cells appear in deeper sections. This neuroanatomy and staining pattern is consistent with that seen in thin frozen sections (Kleinfeld et al., 1994). Although there was a progressive reduction in signal intensity with depth, high spatial resolution images were obtained throughout the preparation with no apparent deterioration of spatial resolution. Field potential recordings taken during TPLSM imaging did not show significant alteration of the intrinsic oscillation, suggesting that there was negligible phototoxicity produced by the imaging procedure.

2.2. Fluorescence imaging of dendrites and synaptic spines of neurons filled with ion indicators in rat hippocampus and turtle cortex

The ability to resolve dendritic structure and synaptic spines using TPLSM was examined by microinjecting single neurons in brain slice preparations with the fluorescent free-calcium-ion indicator Calcium Green (Molecular Probes). Brain slices from rat hippocampus and turtle cortex were examined.

Transverse hippocampal brain slices from PND 13–30-day-old rats were cut at a thickness of $400 \mu\text{m}$ and maintained in a submerged slice chamber. Individual CA1 hippocampal pyramidal cells were filled with Calcium Green by iontophoresis through high-resistance ($80\text{--}150 \text{ M}\Omega$) intracellular microelectrodes (7 mM Calcium Green in 300 mM KCl; -0.5 nA ; 10 min) following procedures previously described for fura-2 imaging (Regehr and Tank, 1992). Following injection, the microelectrode was removed from the cell and the slice was incubated for approximately 30 min to allow the dye to diffuse and fill the dendritic arbor. The slice was then transferred to a submerged slice chamber on the TPLSM and images of filled neurons were obtained using an excitation wavelength of 860 nm and a $63 \times /0.9$ NA Zeiss water immersion objective. Fig. 3A is a low-magnification stereo-image pair of the dendritic tree of a CA1 cell constructed from a set of 72 optical sections taken every $1 \mu\text{m}$. In Fig. 3B, a single optical slice of a short section of dendrite is shown at a higher magnification. Dendritic spines are easily resolved. This section of dendrite was located about $150 \mu\text{m}$ below

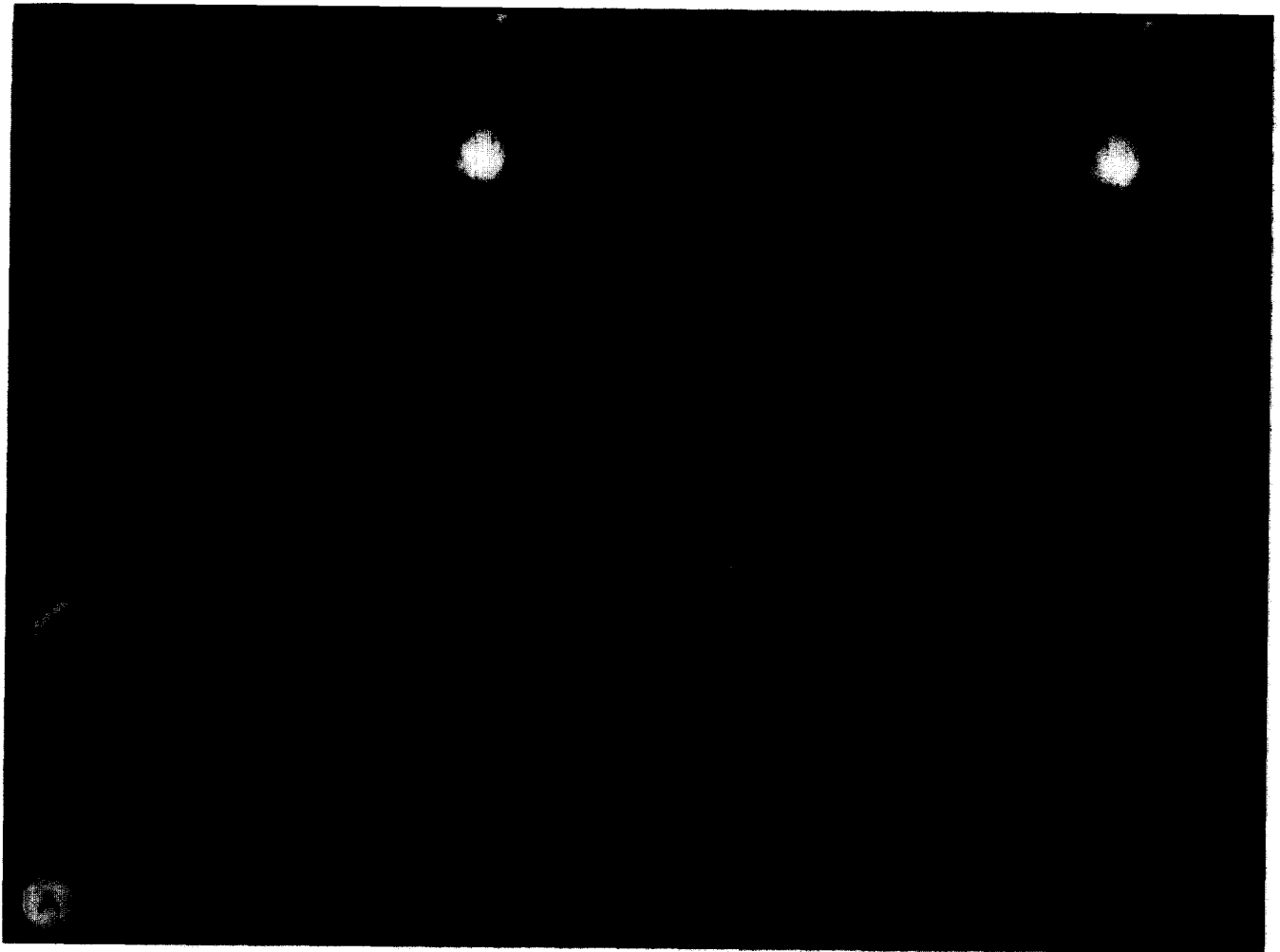
the surface of the brain slice. Images of spines were repetitively taken at this spatial resolution with no obvious signs of photodamage. Although single-photon confocal images of spines have been made at depths of a few to tens of micrometers (Guthrie et al., 1991; Muller and Connor, 1991), images of dendritic spines on living neurons located at these much greater depths in mammalian preparations have not, to our knowledge, been reported. Our images are consistent with the expected improvements in depth penetration using 2-photon excitation.

We also imaged dendritic structure and spines in brain slices from turtle cortex. Coronal slices $400 \mu\text{m}$ thick were prepared from dorsal cortex of *Pseudemys scripta*. Slices were maintained at room temperature in oxygenated amphibian ringer in a submerged slice chamber and individual pyramidal neurons were injected with Calcium Green following the procedures described above for mammalian hippocampus. Prior to imaging with the TPLSM, calcium transients in response to intracellular current injection and stimulation of afferent fibres were examined with a cooled charge coupled device camera using standard procedures (Yuste et al., 1994). The rate of recovery of calcium transients produced by intracellular current injection was about 1 s in the dendrites and several seconds in the soma, indicating that the cells had not been overinjected with calcium indicator. Fig. 3C shows a high-magnification image of a short section of pyramidal cell dendrite located $130\text{--}150 \mu\text{m}$ below the slice surface. A range of dendritic morphologies from small stubs and pedunculated spines to long filiform appendages, about $5 \mu\text{m}$ in length, are clearly visible. The fact that synaptic spines were easily resolved at depths greater than $100 \mu\text{m}$ in both rat and turtle preparations suggests that 2-photon imaging will have general applicability to high-resolution anatomical and functional imaging of dendrites, spines, and other micrometer-sized structures, such as presynaptic nerve terminals.

2.3. Fluorescence imaging of voltage-sensitive dye-labeled cortical brain slice

Two-photon microscopy also can be used to image brain slices labeled with voltage-sensitive dyes. This method has the promise of detecting spatial patterns of activity at cellular resolution without requiring multiple electrode arrays or individually-filled neurons. Here we present preliminary results on the localization of fluorescence from brain slices labeled with two different voltage-sensing dyes.

Conventional transverse slices ($400 \mu\text{m}$ thick) were prepared from the ventral hippocampus of adult rats and allowed to recover for at least 1 h in a static interface holding chamber. Slices were then stained by



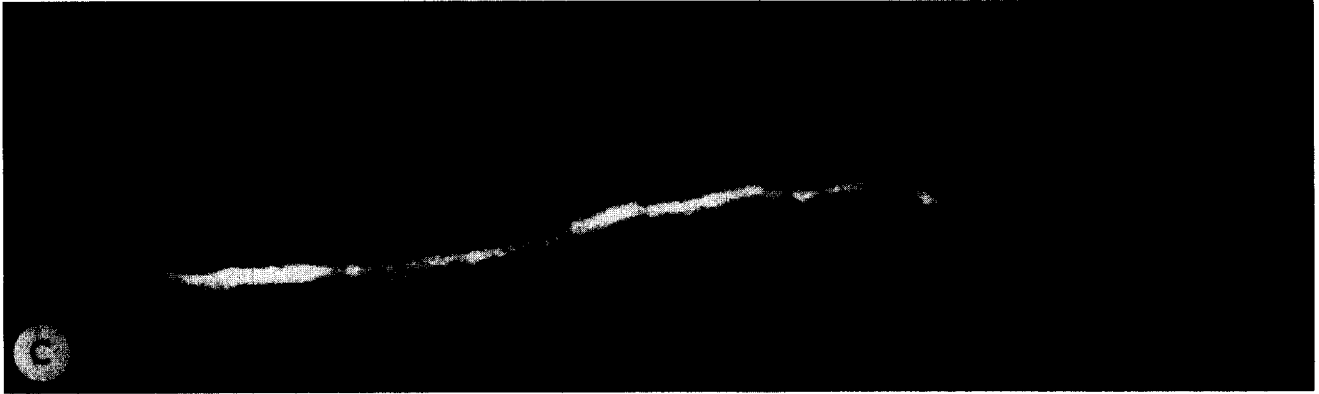


Fig. 3 (continued).

incubation in either RH414 or di4-ANEPPS (5–20 μM in 0.1% ethanol) dissolved in a small volume of normal artificial cerebro-spinal fluid (ACSF) (5–10 ml) for approximately 5 min. The slices were then washed in fresh ACSF for 2 min and placed in a submerged recording chamber. In fluorescence images of the CA1 subfield in these slices we always observed numerous bright small round structures ($< 5 \mu\text{m}$) that might be axonal terminals or myelinated fibers in cross-section (see Fig. 4). The somata and apical dendrites of CA1 pyramidal cells were clearly demarked by the relative absence of fluorescence within them. Images could be made down to a depth of over 100 μm into the slice, whereas fluorescent structures in only the first few tens of micrometers were discernible when examining similarly stained slices with a conventional epi-fluorescence microscope. The preferential staining of small and thin structures suggests that voltage-sensitive dyes may be concentrated in axonal (and perhaps even non-neuronal) structures. This hypothesis is consistent with our observation that regions with very high densities of axons such as the alveus in CA1 and the white matter in neocortex stained much more intensely than neighboring regions dominated by somata and dendritic processes. Physiological studies (Grinvald et al., 1982) also suggest that a large component of the change in

the fluorescence of these dyes in response to synaptic stimulation is presynaptic.

2.4. *In vivo* fluorescence imaging of voltage-sensitive dye-labeled cerebral cortex

Voltage sensitive dyes can be used to record activity from mammalian cortex in whole animal preparations. In studies using conventional imaging, the processed signal corresponds to the spatially averaged transmembrane potential from neurons and glia in layer 1 and the upper part of layers 2/3 (Grinvald et al., 1994; Orbach et al., 1985). There may also be additional contributions to the signal from non-voltage dependent sources (Grinvald et al., 1982). As a first step in exploring the use of 2-photon excitation for *in vivo* cortex experiments, we stained the cortex of juvenile rats with a voltage-sensitive dye and imaged through the pial surface with the TPLSM.

We used the parietal cortex from rat (PND30; 100 g), stained with the dye RH795. In brief, animals were anesthetized with urethane and a bone flap above one hemisphere was removed. The dura was dissected and the underlying cortex was stained with a solution of the

←
Fig. 3. Two-photon fluorescence images of dendrites and synaptic spines from Calcium Green-filled cortical neurons in brain slices. A: stereo-image pair created from TPLSM fluorescence images of a CA1 pyramidal neuron in a hippocampal slice taken from a PND 24 rat. The cell was located 150 μm below the slice surface and was iontophoretically injected with the calcium indicator Calcium Green as described in the text. At the end of the injection the cell had 80 mV action potentials and normal responses to pulses of depolarizing current. The estimated intracellular concentration of the dye was 100–200 μM . Note that dendritic spines can be clearly resolved. B: section of dendrite at higher effective magnification from a Calcium Green labeled CA1 hippocampal pyramidal cell in a 400- μm -thick brain slice. Image size: 41 $\mu\text{m} \times 27 \mu\text{m}$. C: section of dendrite from a Calcium Green-filled pyramidal neuron in a 400- μm -thick brain slice from dorsal cortex of *Pseudemys scripta*. Image size: 61 \times 18 μm .



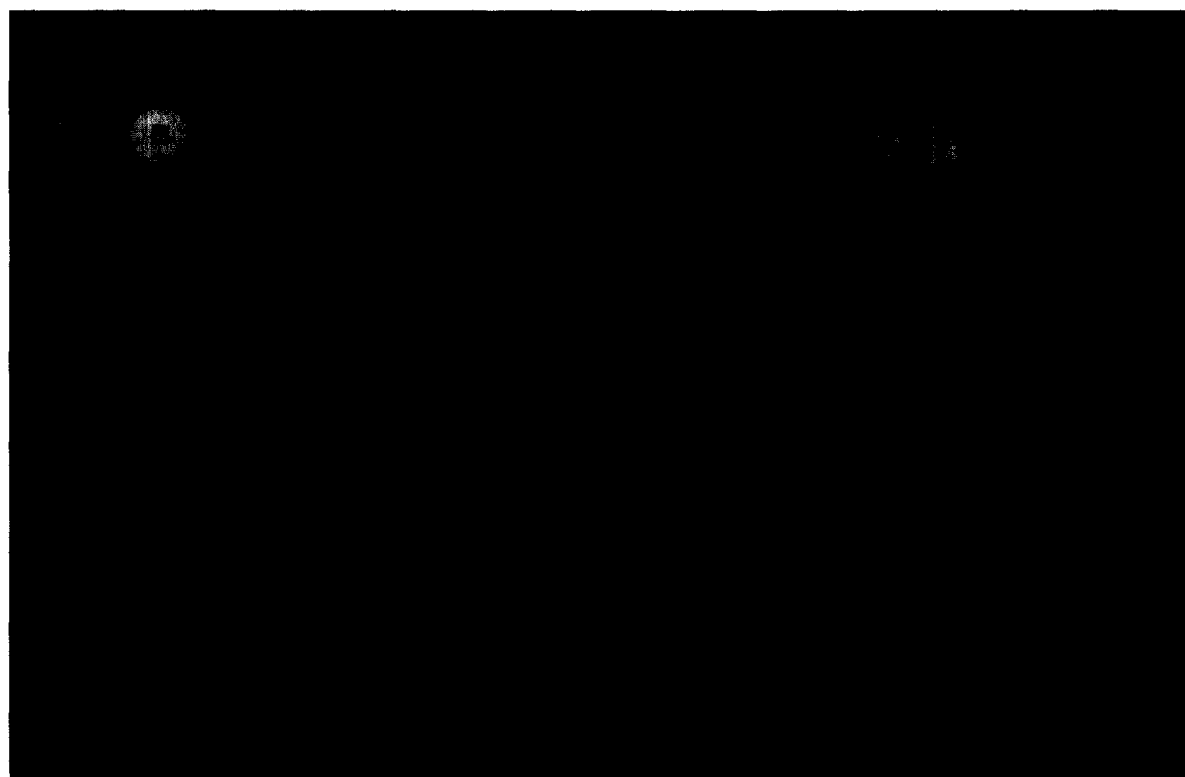
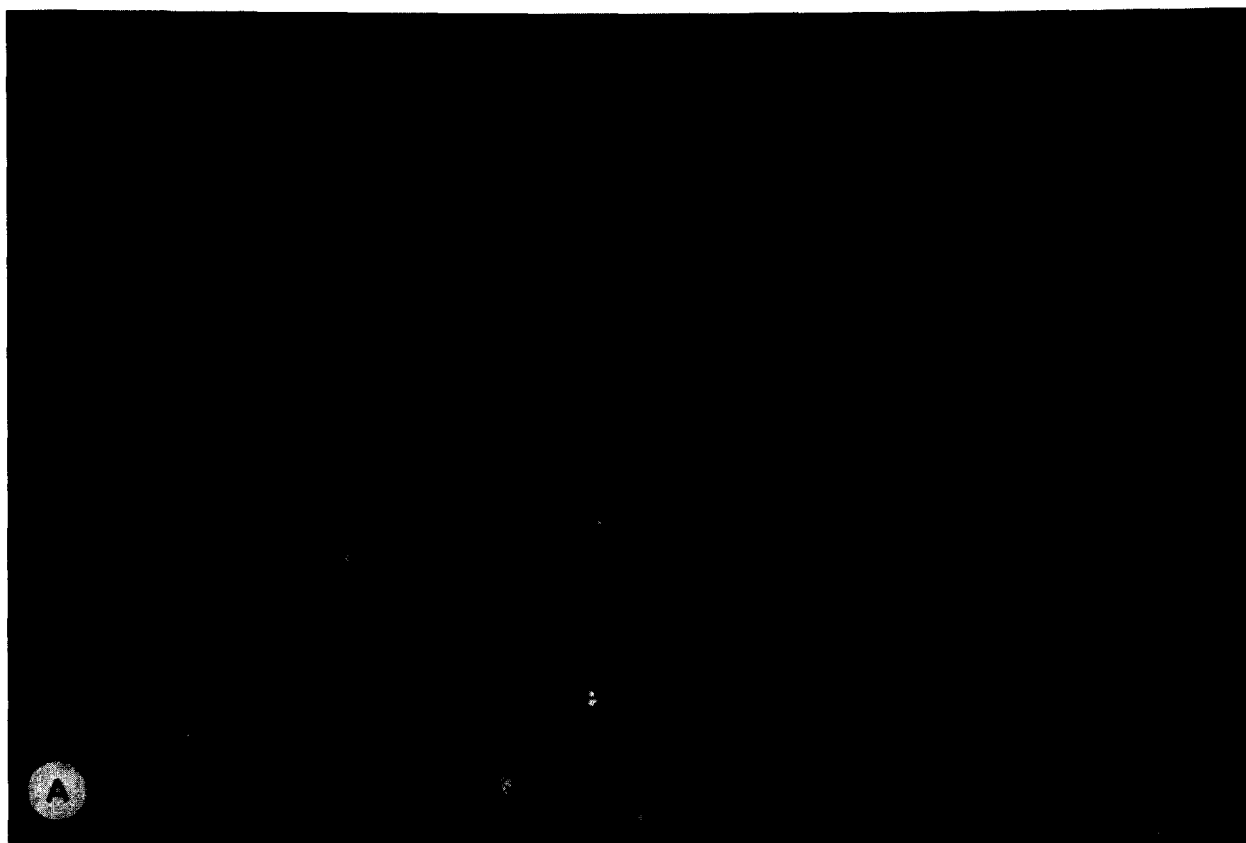
Fig. 4. A: two-photon fluorescence image of the CA1 subfield of a rat hippocampal slice ($400\ \mu\text{m}$ thick) stained with the voltage-sensitive dye RH414 (approximately $15\ \text{mM}$ for $5\ \text{min}$). Neuronal somata and dendrites could be distinguished by the relative absence of fluorescence in these processes. Most fluorescence appeared to emanate from small diameter ($< 10\ \mu\text{m}$) processes and puncta and was brighter in the alveus and st. oriens than in st. pyramidale or st. radiatum. Similar staining patterns were observed with di-4-ANEPPS, a voltage-sensitive dye of different chemical structure, and were visible to a depth of $100\ \mu\text{m}$. These patterns suggest these dyes might be preferentially accumulating in axonal or non-neuronal processes. The optical section thickness is about $1\ \mu\text{m}$. Calibration bar: $25\ \mu\text{m}$.

dye ($0.1\ \text{mg/ml}$ in ACSF for $40\ \text{min}$); this dye has a 1-photon absorption maximum at $500\ \text{nm}$ with a FWHM of $\approx 140\ \text{nm}$. The cortex was covered with low-melting-point agarose and sealed by a cover glass to reduce pulsation. The animal was positioned so that the optical axis of the microscope was perpendicular to the cortical surface. Consecutive tangential sections were

acquired as the focal plane was moved down from the pial surface.

At the cortical surface, we observed the stained walls of vasculature and small stained outlines that correspond to glial limitans (Peters et al., 1991), the appendages of astroglia. From the surface to a depth of about $100\ \mu\text{m}$, only vasculature and occasional

Fig. 5. In vivo fluorescence images of voltage-sensitive dye-labeled rat parietal cortex. A: optical section located $180\ \mu\text{m}$ below the pial surface. The dark circles are the somata of cortical neurons. The obliquely oriented apical dendrite of 1 neuron with is apparent. Image size: 382×256 pixels corresponding to $200 \times 133\ \mu\text{m}$. B: a graph of fluorescence signal intensity (grey levels) versus depth (μm) below the pial surface. Inset: optical xz section taken perpendicular to the cortical surface.



somata were resolved, although significant fluorescence was present. This is consistent with the dense neuropil and sparse cell body density expected in layer 1 of the cortex. At greater depths, dark areas, characteristic of cell somata against a dense background fluorescence of cellular processes, were apparent (Fig. 5A). We occasionally observed a neuron with its primary apical dendrite oriented obliquely and thus transected by the focal plane (Fig. 5A). As in the brain

slice preparation described earlier, we observed many small, strongly stained puncta, which might correspond to myelinated axons or presynaptic terminals. The images obtained from live animals with TPLSM were very similar to what is seen in thin sections prepared from freshly frozen samples of similarly stained tissue (data not shown).

The average intensity of the TPLSM signal as a function of depth is shown in Fig. 5B. The analysis of

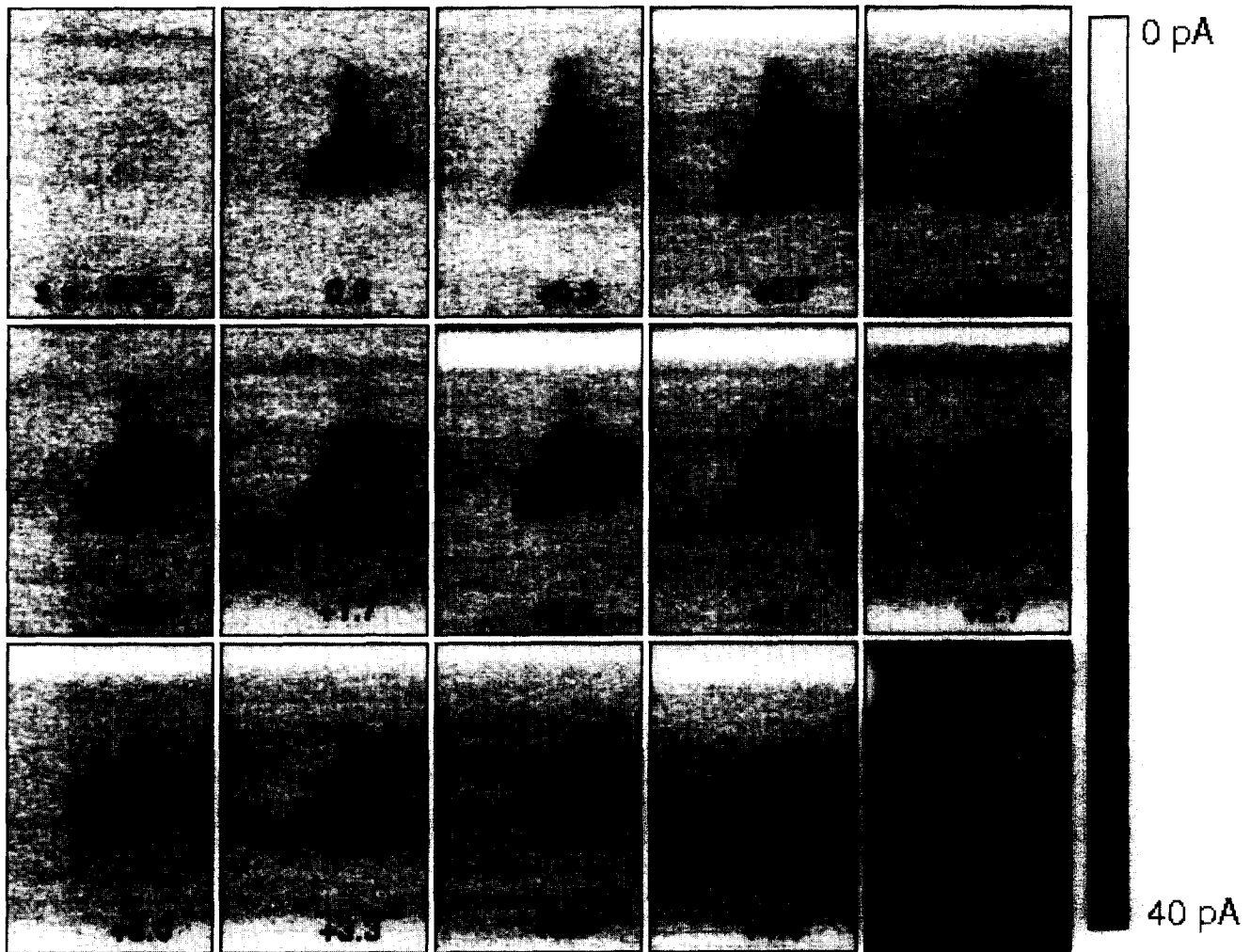


Fig. 6. Nicotinic acetylcholine receptors imaged on a tissue cultured BC3H1 cell with 2-photon SPM and whole-cell current detection (inward current displayed as pixel darkening). Bathing medium with 0.5 mM 'caged' carbamylcholine (CA) was perfused over the cell from the lower left direction using a 200 μm ID capillary (not visible). The optical section properties of 2-photon excited SPM microscopy is demonstrated by a 'through-focus-series' of photo-activated current images. The lack of out-of-focus release of agonist is strikingly evident from the difference between the images at taken with the focal plane position (z) 0.7 μm below the coverslip surface and the large amount of induced current seen for $z = 0.3 \mu\text{m}$. A beam deflection image (Wilson, 1987) taken simultaneously with one of the I_{pa} images, of the cell with the attached recording pipette is shown at an intermediate focal plane position ($z = 2.3 \mu\text{m}$ above coverslip) in the lower left corner. Images were raster-scanned with the fast axis horizontal. Bright stripes visible in the top and/or bottom portions of several images result from the delayed introduction or early withdrawal of the flow of caged compound containing solution over the cell. The current range displayed is 0 to -40 pA . This cell was used on day 7 after plating. The access resistance after establishing whole-cell condition was 12 $\text{M}\Omega$ and rose to 19 $\text{M}\Omega$ towards the end of the experiment. The cell capacitance was 24 pF. Image size: 100 \times 200 pixels corresponding to 50 $\mu\text{m} \times 100 \mu\text{m}$ (adapted from Denk, 1994).

thin sections from similarly stained animals shows that the dye penetrates to a depth of $\approx 500 \mu\text{m}$ in this preparation.

3. Two-photon laser scanning photochemical microscope (SPM)

The principle behind 2-photon SPM (Denk, 1994) is to generate a high concentration of agonist in a small volume by localized photolysis of a bath applied photoactivatable or 'caged' agonist (Lester and Nerbonne, 1982; Adams and Tsien, 1993; Kao and Adams, 1993). If this volume is adjacent to ionotropic cell membrane receptors for that agonist, corresponding ion channels open, in turn admitting current whose magnitude reflects the number of activated receptors at that particular location. The position of the focus of the uncaging laser beam and with it the location of high agonist concentration is scanned across the cell under investigation and the whole-cell current is recorded (Hamill et al., 1981) at the same time. As shown schematically in Fig. 1B, the observed current magnitude at each scan position determines the numerical value of the corresponding pixel. The resulting 'photo-activated' current (I_{pA}) image reflects the receptor distribution on the cell. An example of a set of SPM images of nicotinic acetylcholine receptors on the surface of a tissue cultured BC3H1 cell is shown in Fig. 6. SPM is much faster than iontophoretic mapping, does not require mechanical access for an iontophoresis pipette, and does not generate ejection-current artifacts. In SPM, unlike with binding assays, receptors stay functional and only functional receptors on the electrically accessed cell are detected.

4. Discussion

We have presented anatomical fluorescence images of single neurons and neuronal ensembles in semi-intact and intact nervous systems that resulted from our initial explorations using TPLSM. A quantitative comparison of TPLSM with other imaging techniques such as single-photon confocal microscopy has not yet been performed. However, several important features expected for 2-photon excitation are consistent with the results of our experiments. These are: (1) optical sectioning capabilities with micrometer scale depth resolution, (2) the ability to image at this resolution at depths of more than $100 \mu\text{m}$ below the surface in strongly scattering preparations, and (3) the ability to perform repetitive high-resolution imaging without obvious physiological deterioration.

Although the fluorescence images we presented were anatomical, TPLSM should find applicability in func-

tional imaging of neurons and circuits using ion-sensitive indicators. We have, in fact, observed functional changes in exploratory experiments on dendrites of cortical neurons filled with the calcium indicator Calcium Green. For example in imaging experiments similar to that illustrated in Fig. 3A, image sequences taken at approximately 10 Hz in low- Mg^{2+} saline demonstrated transient increases in Calcium Green signal intensity on primary and secondary dendritic branches of CA1 hippocampal pyramidal cells consistent with transient increases in intracellular free-calcium-ion concentration. Functional imaging of neurons stained with voltage-sensitive dyes may be more difficult because of the much smaller fractional changes in signal fluorescence.

The use of 2-photon excitation to uncage bioactive compounds may be applicable to a variety of problems in neuroscience. The functional SPM image of cell surface neurotransmitter receptor shown in Fig. 6 is complementary to the functional images of larger-scale circuitry in brain slice produced by single-photon laser scanning photoactivation of neurotransmitters coupled with whole-cell patch clamp recording (Callaway and Katz, 1993; Katz, this issue). With 2-photon excitation it is difficult, at the currently available laser power, to liberate large amounts of agonist. Thus 2-photon SPM is less well suited to elucidate connectivity between clusters of neurons. However, due to its higher spatial resolution, both laterally, because of reduced scattering, and vertically, because of optical sectioning, 2-photon SPM should be more useful than 1-photon uncaging in resolving microcircuitry at a single-cell level and below. In particular, the depth discrimination of 2-photon excitation may prove indispensable in performing layer-specific photo-activation in neocortex *in vivo*.

References

- Adams, S.R. and Tsien, R.Y. (1993) Controlling cell chemistry with caged compounds. *Ann. Rev. Physiol.*, 55: 755–784.
- Callaway, E.M. and Katz, L.C. (1993) Photostimulation using caged glutamate reveals functional circuitry in living brain slices. *Proc. Natl. Acad. Sci. USA*, 90: 7661–7665.
- Delaney, K.R., Gelperin, A., Fee, M.S., Flores, J.A., Gervais, R., Tank, D.W. and Kleinfeld, D. (1994) Waves and stimulus-modulated dynamics in an oscillating olfactory network. *Proc. Natl. Acad. Sci. USA*, 91: 669–673.
- Denk, W. (1994) Two-photon scanning photochemical microscopy: mapping ligand-gated ion channel distributions. *Proc. Natl. Acad. Sci. USA*, 91: 6629–6633.
- Denk, W., Piston, D.W. and Webb, W.W. (1994) Two-photon molecular excitation in laser scanning microscopy. In: J. Pawley (Ed.), *The Handbook of Confocal Microscopy*, in press.
- Denk, W., Strickler, J.H. and Webb, W.W. (1990) Two-photon laser scanning fluorescence microscopy. *Science*, 248: 73–76.
- Denk, W., Strowbridge, B., Gelperin, A., Flores, J., Yuste, R., Tank, D.W. and Kleinfeld, D. (1994) Cellular structures are imaged in

- vitro and in vivo with two-photon excited fluorescence. Soc. Neurosci. Abstr., 20: in press.
- Dodt, H.-U. (1992) Infrared videomicroscopy of living brain slices. In: H. Kettenmann and R. Grantyn (Eds.), *Practical Electrophysiological Methods*, Wiley-Liss, New York, pp. 6–10.
- Dodt, H.-U. (1993) Infrared-interference videomicroscopy of living brain slices. *Adv. Exp. Med. Biol.*, 333: 245–249.
- Dodt, H.-U., Hager, G. and Zieglgansberger, W. (1993) Direct observation of neurotoxicity in brain slices with infrared videomicroscopy. *J. Neurosci. Methods*, 50: 165–171.
- Egelhaaf, M., Borst, A., Warzecha, A.K., Flecks, S. and Wildemann, A. (1993) Neural circuit tuning fly visual neurons to motion of small objects. II. Input organization of inhibitory circuit elements revealed by electrophysiological and optical recording techniques. *J. Neurophys.*, 69: 340–351.
- Farber, I.C. and Grinvald, A. (1983) Identification of presynaptic neurons by laser photostimulation. *Science*, 222: 1025–1027.
- Fork, R.L. (1971) Laser stimulation of nerve cells in *Aplysia*. *Science*, 171: 907–908.
- Gelperin, A. and Tank, D.W. (1990) Odor-modulated collective network oscillations of olfactory interneurons in a terrestrial mollusc. *Nature*, 345: 437–440.
- Grinvald, A., Lieke, E.E., Frostig, R.D. and Hildesheim, R. (1994) Cortical point spread function and long range lateral interactions revealed by real time optical imaging of macaque monkey primary visual cortex. *J. Neurosci.*, 14: 2545–2568.
- Grinvald, A., Manker, A. and Segal, M. (1982) Visualization of the spread of electrical activity in rat hippocampal slices by voltage-sensitive optical probes. *J. Physiol. (Lond.)* 333: 269–291.
- Guthrie, P.B., Segal, M. and Kater, S.B. (1991) Independent regulation of calcium revealed by imaging dendritic spines. *Nature*, 354: 76–80.
- Hamill, O.P., Marty, A., Neher, E., Sakman, N. and Sigworth, F.J. (1981) Improved patch-clamp techniques for high-resolution current recording from cells and cell free membrane patches. *Pflügers Arch.*, 391: 85–100.
- Jobsis, F.F. (1977) Noninvasive infrared monitoring of cerebral and myocardial oxygen sufficiency and circulatory parameters. *Science*, 198: 1264–1267.
- Kao, J.P.K. and Adams, S.R. (1993) Photosensitive caged compounds. In: B. Herman and J.J. Lemasters (Eds.), *Optical microscopy. Emerging Methods and Applications*, Academic, San Diego, CA, pp. 27–85.
- Kleinfeld, D., Delaney, K.R., Fee, M.S., Flores, J.A., Tank, D.W. and Gelperin, A. (1994) Dynamics of propagating waves in the olfactory network of a terrestrial mollusc: an electrical and optical study. *J. Neurophysiol.*, 72: 1402–1419.
- Lester, H.A. and Nerbonne, J.M. (1982) Physiological and pharmacological manipulations with light flashes. *Annu. Rev. Biophys. Bioeng.*, 11: 151–175.
- MacVicar, B.A. (1984) Infrared video microscopy to visualize neurons in the in vitro brain slice preparation. *J. Neurosci. Methods*, 12: 133–139.
- Muller, W. and Connor, J.A. (1991) Dendritic spines as individual neuronal compartments for synaptic Ca^{2+} responses. *Nature*, 354: 73–76.
- Orbach, H.S., Cohen, L.B. and Grinvald, A.G. (1985) Optical mapping of electrical activity in rat somatosensory and visual cortex. *J. Neurosci.*, 5: 1886–1895.
- Peters, A., Palay, S.L. and Webster, H.D. (1991) *The Fine Structure of the Nervous System: Neurons and their Supporting Cells*, Oxford Press.
- Regehr, W.G. and Tank, D.W. (1992) Calcium concentration dynamics produced by synaptic activation of CA1 hippocampal pyramidal cells. *J. Neurosci.*, 12: 4202–4223.
- Ross, W.N. and Werman, R. (1987) Mapping calcium transients in the dendrites of Purkinje cells from guinea-pig cerebellum in vitro. *J. Physiol.*, 389: 319–336.
- Sobel, E.C. and Tank, D.W. (1994) In vivo Ca^{2+} dynamics in a cricket auditory neuron: an example of a chemical computation. *Science*, 263: 823–826.
- Stelzer, E.H.K., Hell, S. and Lindek, S. (1994) Nonlinear absorption extends confocal fluorescence microscopy into the ultra-violet regime and confines the illumination volume. *Opt. Comm.*, 104: 223–228.
- Svaasand, L.O. and Ellingsen, R. (1983) Optical properties of the human brain. *Photochem. Photobiol.*, 38: 293–299.
- Tank, D.W., Sugimori, M., Connor, J.A. and Llinas, R.R. (1988) Spatially resolved calcium dynamics of mammalian Purkinje cells in cerebellar slice. *Science*, 242: 773–777.
- Tsien, R.Y. and Waggoner, A. (1992) Fluorophores for confocal microscopy: photophysics and photochemistry. In: J.B. Pawley (Ed.), *Handbook of Biological Confocal Microscopy*, Plenum, New York, pp. 169–178.
- Wilson, T. (1987) Enhanced differential phase contrast imaging in scanning microscopy using a quadrant detector. *Optik*, 80: 167–170.
- Yuste, R., Gutnick, M.J., Saar, D., Delaney, K.R. and Tank, D.W. (1994) Ca^{2+} accumulation in dendrites of neocortical pyramidal neurons: an apical band and evidence for two functional compartments. *Neuron*, 13: 23–43.